MASTERARBEIT / MASTER'S THESIS

Titel der Masterarbeit / Title of the Master's Thesis

„Investigating mSin1 as the potential targeting subunit of mTORC2"

verfasst von / submitted by

Benjamin Lawrence Sinkovics BSc

angestrebter akademischer Grad / in partial fulfilment of the requirements for the degree of

Master of Science (MSc)

Wien, 2017 / Vienna 2017

Table of Contents

Abstract

Although previous research has tied the mechanistic target of rapamycin complex 2 (mTORC2) to cellular growth signaling and survival the investigation of its regulation and function is only at its beginning. The obligate mTORC2 component mSin1 is the prime candidate for targeting mTORC2 localization with its pleckstrin homology (PH) domain which is contained in two of the three mTORC2 forming isoforms. In this study, we examined the localization of eGFP-tagged mSin1 isoforms inside cells by confocal microscopy and investigated the influence of phosphomimetic or phosphomutant mutations of the two AGC kinase motifs within mSin1, T86 and T398 (T362 in isoform 2). We demonstrate that the mSin1 PH domain is necessary for its membrane binding and that phosphorylation of T362, by S6K1, seems to prevent membrane association. Furthermore, we provide evidence which suggests that mSin1-T86 phosphorylation could interfere with nuclear import.

Introduction

The mammalian target of Rapamycin (mTOR) exists in two functionally distinct complexes, mTORC1 and mTORC2. These two complexes share the namesake kinase mTOR and the protein mLST8 and are distinguished by their mutually exclusive scaffold proteins, Raptor in mTORC1 and Rictor and mSin1 (mammalian stress-activated map kinase interacting protein) in mTORC2. Functionally, mTORC1 and mTORC2 couple growth factor signaling with pathways regulating intracellular anabolic functions, such as growth, survival and proliferation (reviewed in Betz and Hall 2013).

While the function of mTORC1 is tightly coupled to its localization (reviewed in Betz and Hall 2013), for mTORC2 the intracellular localization and whether it is important for its activity is largely unknown or controversial. Various reports have shown mTORC2 at different cellular compartments such as the plasma membrane (PM), cytoplasm, endoplasmatic reticulum (ER), mitochondria and the nucleus. The obligate components of yeast TORC2, including the mSin1 ortholog Avo1, were shown to localize to the PM and a population of unknown membrane-proximal vesicles (Berchtold and Walther 2009). Immunofluorescent staining with antibodies against mTOR and Rictor detected little staining at the PM, but suggested a mostly reticular and/or mitochondrial pattern (Betz et al. 2013, Boulbes et al. 2011). In support of the immunofluorescent studies suggesting ER-associated mTORC2 are biochemical fractionation experiments, demonstrating the presence of mTORC2 components and mTORC2-like activity associated with ribosomes (Oh et al. 2010; Zinzalla et al. 2011). Additionally, biochemical fractionation detected mSin1 and Rictor in the ER and cytosolic fractions (Betz et al. 2013, Boulbes et al. 2011) and mTOR, Rictor and mSin1 in cytosolic as well as nuclear fractions (Rosner and Hengstschläger 2008). Interestingly, ER- and mitochondria-localized mTORC2 could actually be at the mitochondria-associated ER membranes (MAM), a domain of the ER, which is tethered to mitochondria, as shown by co-immunofluorescence and fractionation experiments (Betz et al. 2013). Collectively, while many of the previous studies report conflicting data regarding the specific localization of mTORC2 in cells, it appears to localize to the nucleus, cytoplasm and various cellular membrane compartments.

While biochemical fractionation studies have found various mTORC2 components in these compartments, whether mTORC2 is active at these sites within the cellular environment is unclear. Indeed, inside cells, mTORC2 activity at individual compartments

could be counterbalanced by the action of enzymes working on mTORC2 substrates in reverse (e.g. phosphoserine/phosphothreonine phosphatases). Furthermore, immunofluorescence data do not necessarily reflect the activity of the complex inside cells. In order to overcome these challenges, we have recently developed a reporter of endogenous mTORC2 activity in cells (Ebner, Sinkovics et al. 2017). We show that mTORC2 activity in cells is concentrated at the plasma membrane, mitochondria and endosomal vesicles. These data are further supported by the localization of GFP-tagged mSin1, which displayed accumulation at the plasma membrane and a subpopulation of endosomal vesicles (Ebner, Sinkovics et al. 2017; Schroder et al. 2007; Yuan et al. 2015). However, how mTORC2 intracellular localization is regulated remains unclear.

mSin1 is the only obligate mTORC2 subunit with a distinct membrane binding pleckstrin homology (PH) domain. It is therefore likely that mSin1 mediates membrane binding of mTORC2. Indeed, in yeast, truncation of the PH domain in Avo1 resulted in loss of haploid cell viability, while replacement of the PH domain with a different membrane anchor restored survival (Berchtold and Walther 2009). Additionally, research in BHK cells showed the loss of EGFP-mSin1 membrane binding if it lacked the PH domain (Schroder et al. 2007). Furthermore, membrane translocation of the mTORC2 substrate Akt is required for its phosphorylation on the mTORC2 site Akt-S473 (Ebner, Sinkovics et al. 2017), suggesting that mTORC2 is plasma membrane-localized.

The lipid-binding specificity of the mSin1 PH domain remains a subject of some debate. While one study reported binding of mSin1 to phosphatidylinositides and phosphatidic acid (Schroder et al. 2007), another showed mSin1 to bind predominantly to PI(5)P, PI(3,5)P_2, PI(4,5)P_2, PI(3,4,5)P_3, and phosphatidic acid and not the other phosphatidylinositides (Liu et al. 2015). In any case, mSin1 binds to membranes and seems to be the membrane-targeting subunit of mTORC2.

In cells mSin1 is expressed as several splicing isoforms, of which isoforms 1, 2 and 5 (henceforth referred to as mSin1.1, mSin1.2 and mSin1.5 respectively) have been shown to form functional mTORC2s (Frias et al. 2006). Isoforms 1 and 5 mRNAs seem to be expressed in most human tissues with the heart and skeletal muscle displaying the highest expression, especially of isoform 5 (Schroder et al. 2004). Notably, the difference in the molecular weight between isoform 1 and 2 is minor and that could be the reason as to why it was not detected in the above-mentioned study. Additionally, the expression of at least mSin1.1 and

mSin1.2 was reported in several cancer cell lines (Schroder et al. 2005, Frias et al. 2006). To our knowledge, up to date, protein expression of isoform 5 *in vivo* has not yet been reported. It is an intriguing possibility that the mSin1 isoforms, which determine the distinct mTORC2s, could serve distinct intracellular roles, especially as isoform 5 lacks the PH domain. Furthermore, mTORC2 containing mSin1.5 had a higher basal kinase activity than that defined by isoforms 1 or 2, and, compared to mSin1 isoforms 1 and 5, the activity of mTORC2 defined by isoform 5 was not significantly increased upon insulin stimulation (Frias et al. 2006). The existence of multiple splice variants of mSin1, their incorporation into distinct mTORCs, and their differential localization leads to the possibility that mTORC2 is compartmentalized at least in part by mSin1. However, the mechanisms responsible for regulation of mSin1 membrane binding and its nuclear accumulation inside cells are not known.

There is not much data on the nuclear function of mSin1 or mTORC2. The most comprehensive study investigated the nuclear and cytoplasmic distribution of the mTORC complexes by subcellular fractionation (Rosner and Hengstschläger 2008). They found that mTORC2 components were more abundant in the cytoplasm than the nucleus in NIH3T3 cells (Rosner and Hengstschläger 2008). Additionally, 24 h treatment with rapamycin (the namesake drug of mTOR, which inhibits mTORC1 under short term and mTORC2 under long-term treatment) promoted mSin1.1 localization in the cytoplasm, at the same time increasing its electrophoretic mobility (Rosner and Hengstschläger 2008). Interestingly, multiple studies reported electrophoretic mobility of mSin1 to be noticeably lower than predicted from the molecular weight of the protein (Schroder et al. 2005; Frias et al. 2006; Liu et al. 2013; Ebner, Sinkovics et al. 2017), presumably indicating heavy posttranslational modification.

As mTORC2 and mSin1 play their part in signaling pathways, it is likely that they are regulated by phosphorylation events. mSin1 contains two AGC-kinase consensus sequences, with both the T86 and T398 phosphorylation sites having been reported previously (Liu et al. 2013; Humphrey, Yang et al. 2013; Yang et al. 2015). The studies investigating T86 phosphorylation proposed a model where mSin1-T86 phosphorylation leads to increased activity of mTORC2 towards Akt-S473 (Humphrey, Yang et al, 2013; Yang et al. 2015). In contrast, Liu et al. (2013), reported that T86 phosphorylation leads to reduced mTORC2 activity and simultaneous phosphorylation of both mSin1 T86 and T398 resulted in mTORC2

disassembly. These conflicting data regarding the function of mSin1 phosphorylations prompted us to further examine their effects on intracellular localization and regulation of mTORC2.

Here, we used a combination of microscopy and supporting biochemical experiments in human cancer cell lines to examine how phosphorylation of mSin1 affects its intracellular localization at membrane compartments and in the nucleus.

Results

The PH domain determines membrane binding of mSin1

mSin1 has multiple splicing isoforms (Figure 1A) of which isoforms 1, 2 and 5 form distinct functional mTORC2 complexes (Frias et al. 2006). In order to investigate the localization of mSin1 in cells, we generated C-terminally eGFP-tagged human mSin1 constructs. The C-terminal tag was chosen because a previous study reported that C- but not N-terminally myc-tagged mSin1 incorporated into functional mTORC2 (Frias et al. 2006), suggesting that the N-terminus is important for complex formation. We then transiently transfected HeLa, HEK293T and Mcf-7 cells with eGFP-tagged mSin1 isoforms 1, 2 and 5 (mSin1.1, -1.2 and -1.5), fixed the cells, and examined the intracellular localization of the Sin1 isoforms using confocal microscopy (Figure 1B). mSin1.1 (the full length isoform) localized throughout the cell with notable accumulation at the plasma membrane (PM), in the nucleus, cytoplasm and vesicular structures. With the exception of HEK293T cells, where Isoform 2 displayed a reduced nuclear signal, mSin1.2, which lacks a short central region, localized similarly to isoform 1 but displayed somewhat stronger accumulation at membrane compartments. Importantly, mSin1.5, which lacks the C-terminal lipid binding pleckstrin homology (PH)-domain did not accumulate at the PM nor vesicles while retaining nuclear and cytoplasmic localization. The results for mSin1.1 and 1.2 in HeLa cells are consistent with previously published results (Yuan et al. 2015). mSin1.5 localization is supported by previous reports showing that GFP-Sin1ΔPH localized to the nucleus and cytoplasm in BHK cells (Schroder et al. 2007). Consistently, Flag-tagged Sin1.5 displayed a similar localization in DG75 cells (Schroder et al. 2004). In agreement with these results, in our recently published paper we demonstrated mSin1.2 co-localization with membrane compartment markers in HEK293T cells with high resolution using structured illumination microscopy (SIM) (Ebner, Sinkovics et
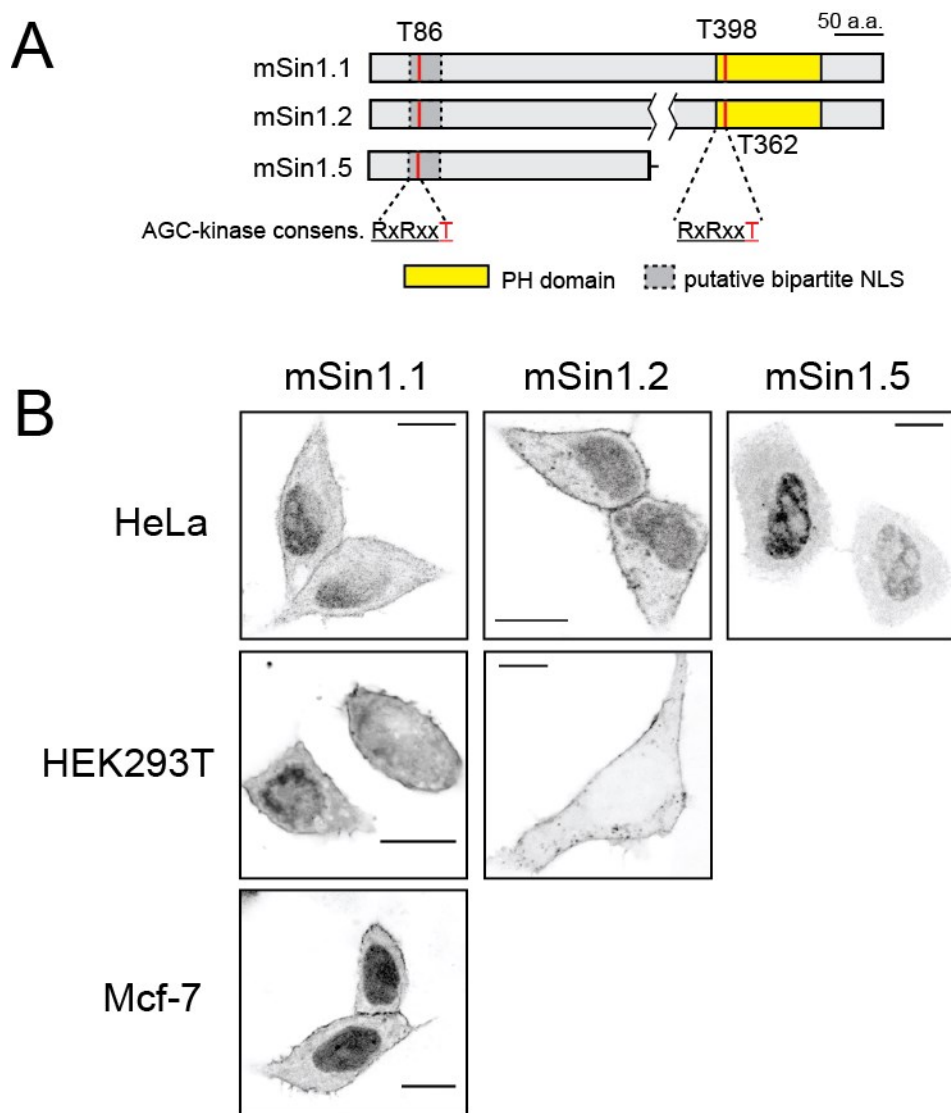
Figure 1: **mSin1 Isoforms show differential localization**

A. Schematic protein representation of the three mSin1 splicing Isoforms 1/2/5. Red lines denote the indicated phosphorylation sites.

B. mSin1-GFP isoform localization depends on the presence of the PH the domain: Confocal laser microscopy images of fixed HeLa cells transiently transfected with mSin1-GFP isoforms or GFP only control (Bars = 5μm). mSin1.2 in HEK293T cells was also co-transfected with mCherry tagged Rab7 (not shown here), and this particular experiment (mSin1.2 in HEK293T cells) was conducted by Ivan Yudushkin.

Parts of these data/figures were already published in Ebner, Sinkovics et al. (2017).

al. 2017). Unlike the previous reports, suggesting presence of mTORC2 at the ER and mitochondria (Boulbes et al. 2011, Betz et al. 2013), we did not detect mSin1 at those compartments. mSin1.2 co-localized with the plasma membrane marker as well as the early- and late endosomal markers (Ebner, Sinkovics et al.2017). Taken together, these data indicate that the localization of mSin1 is isoform-specific and that the PH domain is required for its membrane binding.
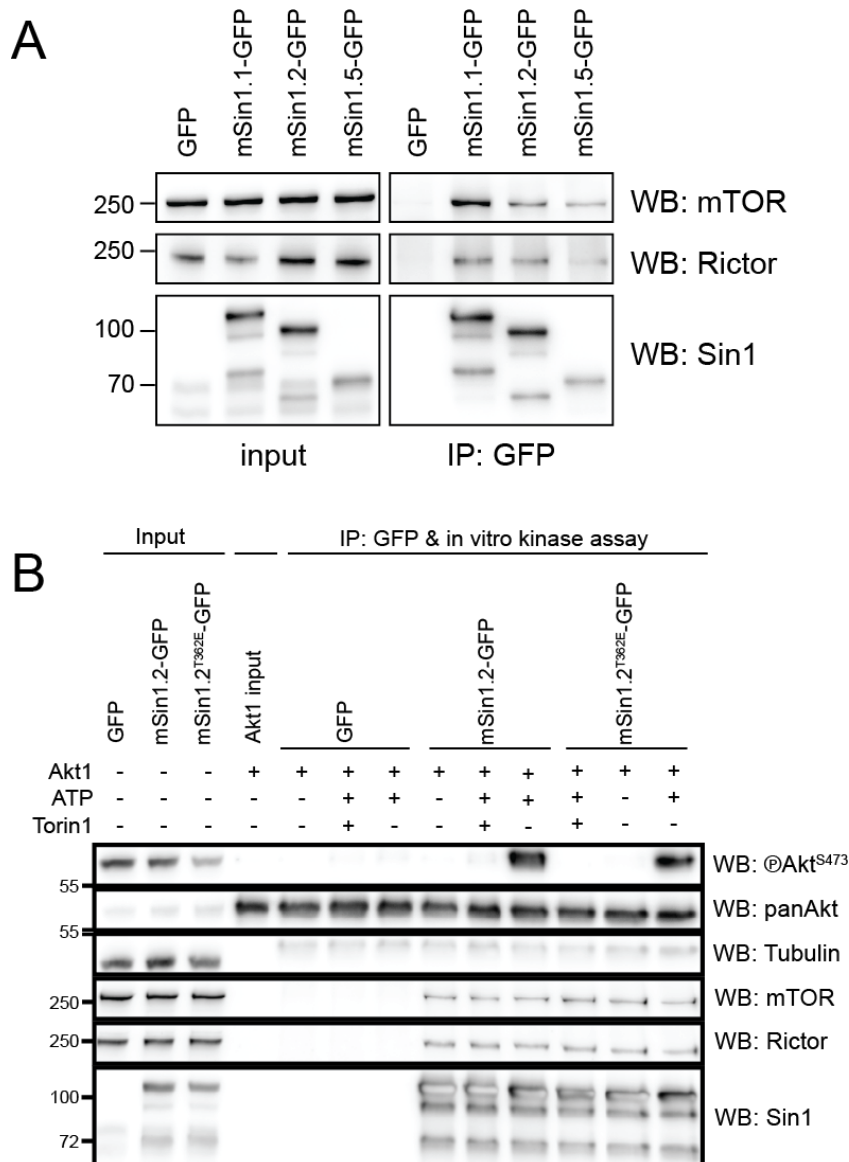
Figure 2: **GFP fusions of mSin1 isoforms 1, 2 and 5 are incorporated into functional mTORC2**
A: mSin1-GFP isoforms 1, 2 and 5 are part of mTORC2: GFP-Trap® pull downs of mSin1 isoforms from transiently transfected HEK293T cells analysed by western blotting. Shown is a representative result with mSin1.1 and mSin1.5 having n=2, and mSin1.2 n=3 respectively.
B: mSin1.2T362E mutation in the PH domain does not interfere with formation of active mTORC2. GFP-Trap® pull downs of mSin1.2-GFP from transiently transfected, non-starved but insulin induced HEK293T cells was followed by an in vitro kinase assay of the full length dephosphorylated AKT1 and analysis by western blotting. Shown is a representative result with n=2.
Parts of these data/figures were already published in Ebner, Sinkovics et al. (2017).

The used eGFP tag could inhibit complex formation or interfere with mTORC2 assembly due to non-stoichiometric expression of mSin1-GFP. In order to test whether mSin1-GFP constructs are able to incorporate into mTORC2, we performed immunoprecipitation experiments. HEK293T cells were transiently transfected with mSin1.1, -1.2 or -1.5 eGFP-tagged constructs, grown for 24 h and lyzed in CHAPS-containing buffer,

which preserves complex integrity (Sarbassov et al. 2004; Frias et al. 2006). mSin1 was pulled down by single-chain anti-GFP antibodies (GFP-Trap®), and input- and bound fractions were analyzed by SDS-PAGE and Western blotting (WB). All three GFP-tagged mSin1 isoforms (1, 2 and 5) were able to co-immunoprecipitate (IP) the obligate mTORC2 components Rictor and mTOR (Figure 2A). Our results are in line with a previous report showing the pull-down of mTORC2 components by myc-tagged mSin1 Isoforms 1, 2 and 5 (Frias et al. 2006). Importantly, these results indicate that neither the C-terminal GFP tag nor the lack of the PH domain interfere with mTORC2 complex formation.

Phosphorylation of the mSin1 PH domain by S6K1 could inhibit membrane binding

As we demonstrated above, the PH domain is required for mSin1 membrane binding, yet dispensable for mTORC2 formation. A recent study (Liu et al. 2013) proposed that AGC kinases, such as S6K or Akt, could phosphorylate T86 and T398 in mSin1. We noticed that T398 (T362 in mSin1.2) is in the PH domain of mSin1. The published crystal structure of the mSin1 PH domain (Pan and Matsuura, 2012) demonstrated that T398 is located close to the lipid-binding basic patch on the surface of the PH domain. We therefore hypothesized that introducing a negative charge close to this lipid-binding surface in the PH domain could interfere with mSin1 membrane binding.

In order to test this hypothesis, we first compared the localization of GFP-tagged mSin1.2 phosphomimetic T362E mutant with the wild type mSin1.2^{WT}. HeLa cells were transiently co-transfected with mSin1.2-eGFP and mCherry-KRas4B^{C30} as a plasma membrane marker, fixed, and examined using confocal microscopy (experiment was conducted by Ivan Yudushkin). The localization of the T362E phosphomimetic mutant was similar to that of mSin1.5-eGFP, as it accumulated in the cytosol and nuclei and was absent from membrane structures (Figure 3A). The WT protein co-localized with the plasma membrane marker, as expected. These results indicate that phosphorylation of T398/T362 in the PH domain could result in displacement of mSin1 from membranes and therefore regulate mTORC2 membrane targeting.

In order to confirm that the phosphomimetic T362E mutation does not interfere with formation of functional mTORC2 complex we performed pull downs on insulin treated HEK293T cells and used the IP fractions for an *in vitro* kinase assay with purified full length dephosphorylated Akt1 as substrate (Figure 2B). Both mSin1.2-eGFP WT and the T362E
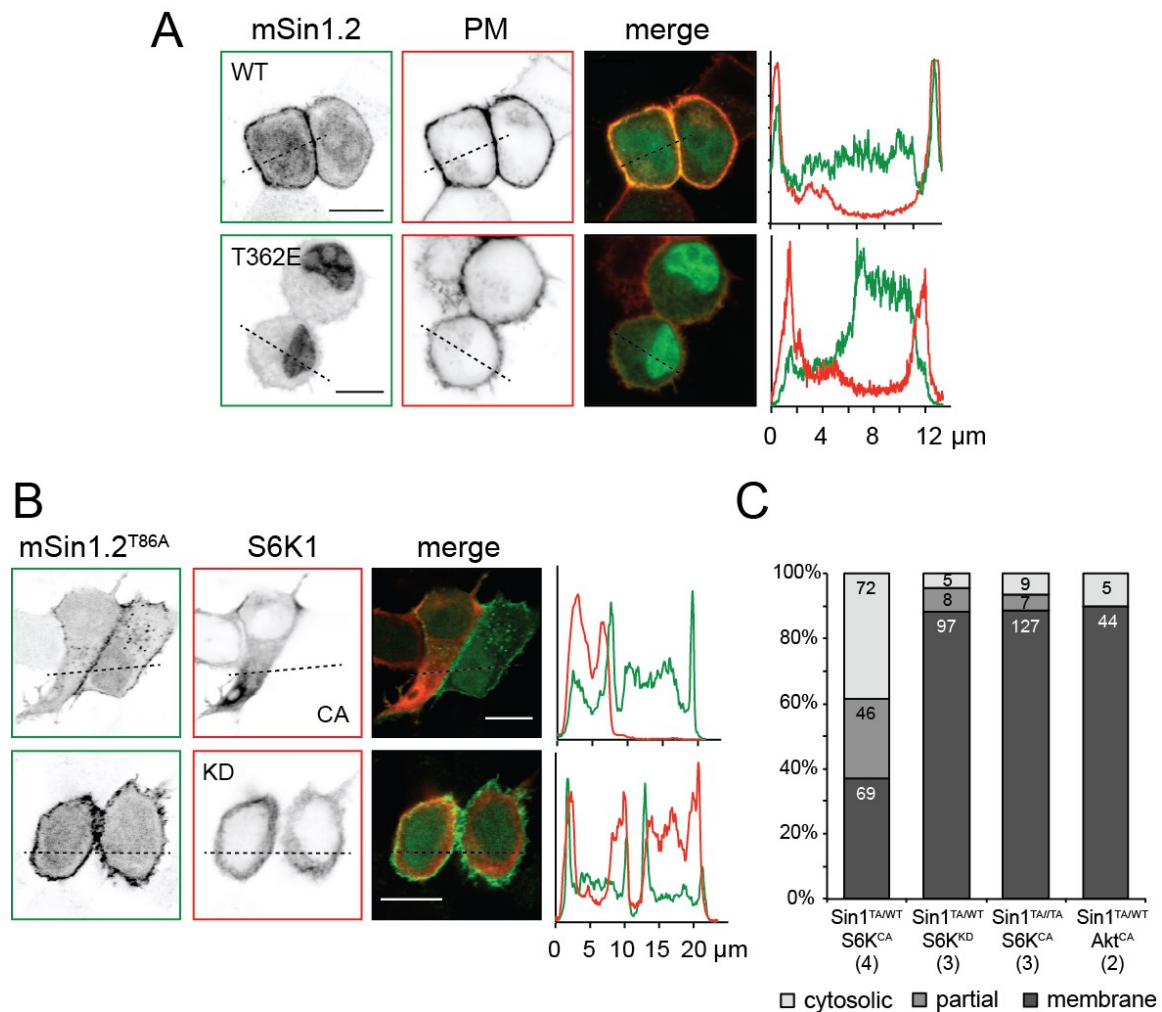
Figure 3: **mSin1 PH domain phosphorylation could displace mTORC2 from the plasma membrane**

A. The phosphomimetic mSin1T362E does not accumulate at the plasma membrane. Confocal laser microscopy images of fixed HeLa cells transiently co-transfected with mSin1-GFP constructs and plasma membrane marker mCherry-KRas4BC30 (Bars = 5µm). The fluorescence intensity profiles display the fluorescence intensity across the indicated line (orientation from left to right). This experiment was conducted by Ivan Yudushkin.

B.These experiments were conducted jointly with the lab intern Sabine Hallamasek (Clare College, Memorial Court, CB3 9AJ Cambridge (UK)). Left: Co-expression of constitutively active S6K results in mSin1.2T86A displacement from the plasma membrane. Immunostainings of fixed HeLa cells transiently co-transfected with mSin1.2T86A-GFP and HA-tagged constitutively kinase active (CA) or inactive (KD) S6K. The fluorescence intensity profiles display the fluorescence intensity across the indicated line (Bars = 10µm).

C. Blind fashion quantification of exeriments as shown in B. Immunostainings of fixed HeLa cells transiently co-transfected with mSin1.2T86A-GFP (Sin1TA/WT) or mSin1.2T86A/T362A -GFP (Sin1TA/TA) as control and HA-tagged constitutively kinase active (CA) or inactive(KD) S6K1/Akt1 were quantified in a blind fashion into the three groups, clear cytosolic localization/partial membrane localization/ clear membrane localization. The numbers in brackets indicate the individual experiments conducted while the numbers within the bars indicate individual number of cells.

phosphomimetic mutant were a part of full mTORC2, co-immunoprecipitating with both Rictor and mTOR, indicating that T362E does not interfere with complex formation. Furthermore, both WT and the T362E mutant displayed kinase activity towards the mTORC2

substrate Akt1-S473, in the presence of ATP. Torin1, a specific mTOR kinase inhibitor, inhibited the kinase activity demonstrating that the activity of the pull down fractions is mTOR-dependent (Figure 2B). These results indicate that the phosphorylation in the mSin1 PH domain, which prevents mSin1 from membrane binding, does not interfere with complex integrity or activity.

In order to examine which of the AGC kinases could phosphorylate the T362 site in cells, we co-transfected HeLa cells with either constitutively active (CA) S6K1 or Akt1 kinases, which were proposed to phosphorylate this site (Liu et al. 2013), and mSin1.2^{T86A}-eGFP. The mSin1-T86 site was always mutated to alanine in order to remove the possibility of phosphorylation and thus secondary effects. The cells were fixed, permeabilized, blocked, treated with anti-HA and anti-mouse Alexa Fluor® 647-conjugated antibodies for Akt/S6K visualization. Images were acquired by confocal laser microscopy and cells were classified in a blinded manner either as displaying clearly <u>cytosolic</u>, <u>partial</u> membrane binding or clear <u>membrane</u> localized according to the localization of transfected mSin1.2^{T86A}-eGFP constructs (Figure 3B). These experiments were conducted jointly with the lab intern Sabine Hallamasek (Clare College, Memorial Court, CB3 9AJ Cambridge (UK)). The cells expressing S6K-CA displayed an almost equal distribution of mSin1.2 into the three groups. In contrast, in the kinase dead S6K expressing cells, mSin1^{T86A} was localized to the plasma membrane in almost 90% of cells. Similarly, primarily membrane association was observed upon co-expression of S6K-CA with the mSin1^{T362A} non-phosphorylatable mutant, suggesting that phosphorylation of T362 in the PH domain by S6K1 could result in displacement of mSin1 from cellular membrane structures. Notably, co-expression of the constitutively active myristoylated Akt1 did not displace mSin1^{T86} from the plasma membrane, suggesting that S6K1, but not Akt1 is responsible for phosphorylation of this site, in agreement with the conclusion from a previous report (Liu et al. 2013). Taken together, our data indicate that mSin1 phosphorylation in the PH domain could result in displacement of mTORC2 from cellular membranes without affecting complex assembly. Thus, this phosphorylation may play a regulatory role in mTORC2 localization.

Here we demonstrated the importance of the mSin1 PH domain for membrane binding and propose that phosphorylation of the AGC kinase motif within this PH domain could displace mSin1 and/or mTORC2 from the membrane and/or prevent it from binding to it.

mSin1 Threonine 86 phosphorylation could regulate nucleo-cytoplasmic shuttling of mSin1

We noticed that in addition to its membrane localization, mSin1-eGFP also localizes to the cytosol and nucleoplasm in interphase cells. The nucleo-cytoplasmic distribution often varied between cells, implying some sort of regulatory mechanism, although whether and how this distribution is regulated is currently unknown.

Nucleo-cytoplasmic distribution of many proteins is regulated by means of specific nuclear localization signals (NLS) within their sequence (reviewed in Lange et al. 2007). A previous study (Schroder et al. 2004) has identified a bipartite nuclear localization sequence (NLS) motif in the N-terminal region of mSin1. Furthermore, we noticed that T86, the second AGC kinase phosphorylation site in mSin1, which is supposed to be phosphorylated by either Akt (Yang et al. 2015) or S6K (Liu et al. 2013), lies within this bipartite NLS (Figure 1A). We therefore hypothesized that phosphorylation of this site could prevent its binding to the nuclear import machinery (specifically, importin-α) and thus reduce nuclear import of mSin1 and, possibly, mTORC2.

To test this hypothesis, we transiently transfected HeLa and immortalized mouse embryonic fibroblasts (MEF) cells with either WT, phosphomutant T86A or phosphomimetic T86E mSin1.1/1.2-eGFP mutants, fixed them with formaldehyde, stained with DAPI and examined their intracellular localization using confocal laser microscopy. We then determined the ratio of average eGFP intensity in the nucleus and in the cytoplasm (Nuc:Cyt) in the confocal plane (Figure 4). For the phosphomimetic T86E mSin1 mutant, the Nuc:Cyt ratio was significantly (p<0.001) reduced compared to the wild type and phosphomutant T86A mSin1.1 in both cell lines. Compared to mSin1 isoform 1, mSin1.2 displayed a much lower Nuc:Cyt ratio in both HeLa and MEF cells, although, similar to mSin1.1, in HeLa cells T86E phosphomimetic also showed a significantly decreased nuclear accumulation. In MEF cells, we did not detect statistically significant difference between Nuc:Cyt ratio for mSin1.2^{WT} and the T86E phosphomimetic. Interestingly, in HEK293T cells, mSin1.2, but not mSin1.1, was largely excluded from the nucleus (Figure 1B), indicating that isoform 2 displays distinct intracellular localization, although the reasons for such specificity are currently unclear. The finding that the mSin1-T86E phosphomimetic mutant displayed a reduced Nuc:Cyt ratio, at least for isoform 1, suggests that phosphorylation of T86 could interfere with nuclear import of mSin1 and/or mTORC2.
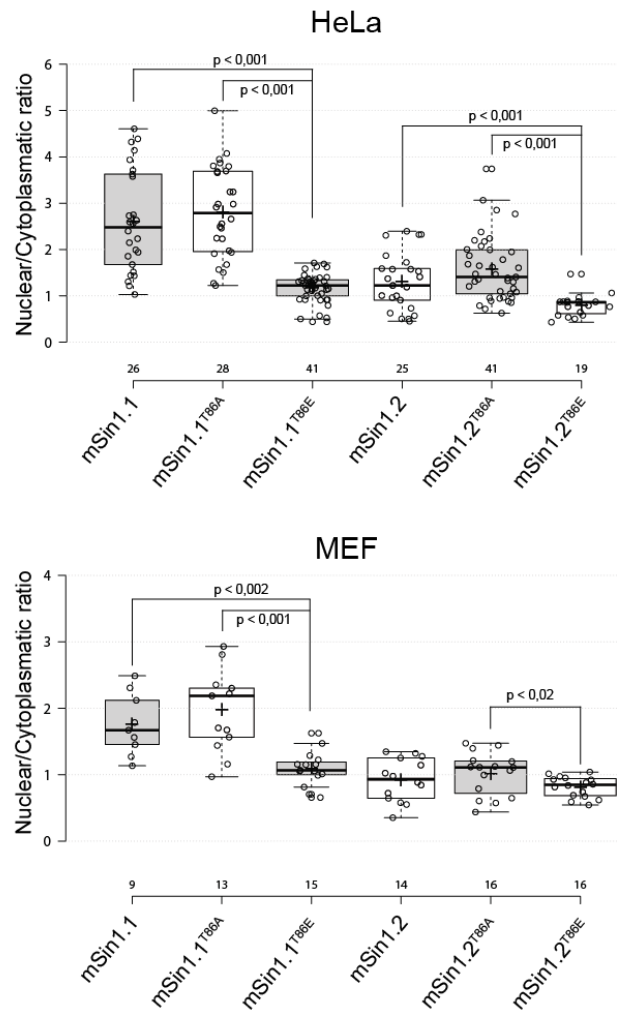
Figure 4: **mSin1 Nuclear/Cytoplasmic distribution is affected by T86 phosphomimetic mutation**
HeLa and MEF cells were transiently transfected with either mSin1.1 or mSin1.2 coupled to GFP as WT or with A T86A / T86E mutation, fixed, stained with DAPI and imaged by confocal laser microscopy. Shown is the quantification of nuclear/cytoplasmica ratio of the average mSin1.x-GFP signal intensity in a single experiment (n=1) with indicated number of analyzed cells. For details see methods section. p-values were calculated by a one tailed t-Test: Two-Sample Assuming Unequal Variances. Non-significant results are not displayed. The box whisker plot was created with: http://boxplot.tyerslab.com/ (Spitzer et al. 2014). Center lines show the medians; plus signs indicate the sample means; box limits indicate the 25th and 75th percentiles as determined by R software; whiskers extend 1.5 times the interquartile range from the 25th and 75th percentiles (Tukey), individual cell ratios are represented by dots and the numbers below bars present the n of cells.

mSin1 Threonine 86 phosphorylation could correlate with Akt-S473 phosphorylation and be dependent on the cell cycle

A previous report indicated that Akt activation and its S473 phosphorylation correlated with cell cycle progression (Liu et al. 2014). Recent publications proposed that Akt is the kinase responsible for T86 phosphorylation (Humphrey, Yang et al. 2013 and Yang et al. 2015). As we also noticed different cellular distributions of mSin1 from cell to cell we hypothesized

that mSin1 phosphorylation on the T86 site, and thus intracellular localization, could also correlate with the cell cycle in an Akt-dependent fashion.

To test this hypothesis, we performed three preliminary experiments. First, we synchronized HeLa, Mcf-7 and MEF cells by double thymidine block, which arrests cells in the early S-phase, and investigated the progression of endogenous mSin1-T86 and Akt-S473 phosphorylation in the cell cycle after release from the thymidine block by subsequent western blot analysis (Figures 5 and 6). Western blots and their quantifications are shown in Figure 5, and the correlation analysis of Akt-S473 and mSin1-T86 phosphorylation, or suspected non-correlating proteins such as panAkt / γ-tubulin or panAkt/mSin1, according to the linear model are shown in Figure 6. In MEF cells, mSin1.1-T86 and Akt-S473 phosphorylation correlated linearly to a high degree (R^2=0.95) compared to the panAKT/γ-tubulin control (R^2=0.07) (Figure 5A and 6A). Interestingly, the phosphorylation of both mSin1.1-T86 and Akt-S473 decreased over the 24 hours after the release from the thymidine block. In HeLa cells, on the other hand, phosphorylation of both mSin1 on T86 and Akt on S473 generally increased and partially correlated with each other along the cell cycle in two independent experiments (Figure 5B and C and 6B and C). Interestingly, in one of the experiments with HeLa cells, mSin1.1-T86 phosphorylation was elevated to a higher level than mSin1.2-T86 (Figure 5B and 6B), while in the second experiment it was the other way around (Figure 5C and 6C). In both experiments the R^2 of the elevated mSin1 isoform was higher than the control (Akt-S473/mSin1.1 R^2=0.30 compared to panAKT/γ-tubulin R^2=0.01 and Akt-S473/mSin1.2 R^2=0.56 compared to panAKT/γ-tubulin R^2=0.39 respectively, although the difference was not as striking as in MEFs (Figure 6B and C). Similarly, in Mcf-7 cells, the phosphorylation of mSin1-T86 and Akt-S473 again displayed a weak correlation with a R^2 of 0.45 compared to the control panAKT/mSin1 R^2=0.16 (Figure 5C). Currently it is impossible to draw any definitive conclusions from these experiments due to their low statistical power, yet the observed correlation between phosphorylation of Akt and its potential substrate mSin1, albeit weak, warrants further investigation.

As we already reported above, the T86E phosphomimetic mutation reduced nuclear accumulation of mSin1.2-eGFP. Together with the possibility that T86 phosphorylation correlates with the cell cycle similar to Akt-S473 phosphorylation, we hypothesized that nuclear import of mSin1 would likely be inhibited during specific cell cycle stages. To test this, we transfected HeLa Kyoto cells, stably expressing H2B-mCherry, thereby allowing the
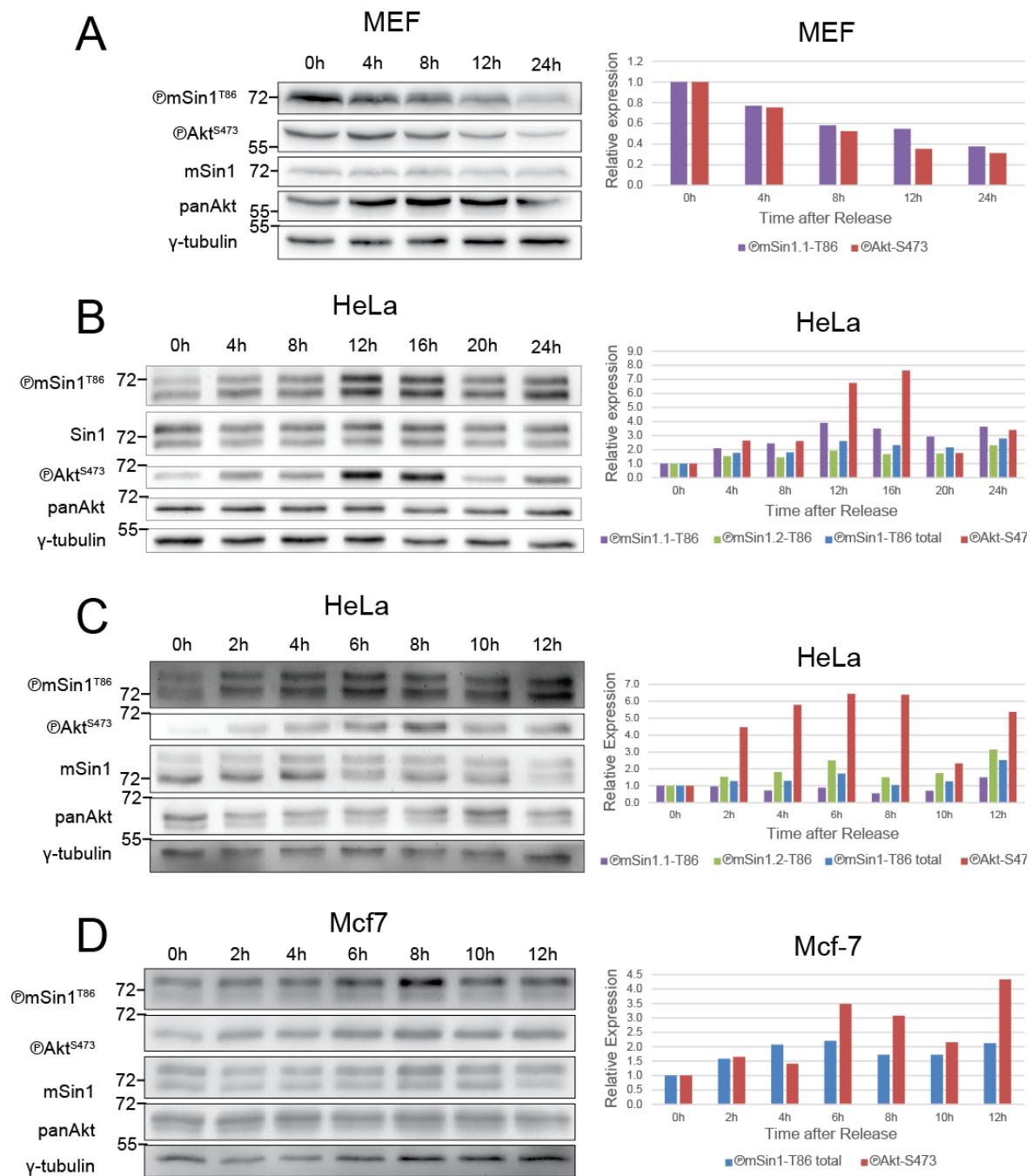
Figure 5: **Phosphorylation of mSin1-T86 and Akt-S473 appear to correlate during the cell cycle**
MEF (A). HeLa (B&C) and Mcf-7 (D) cells were arrested in the G1/S phase by double thymidine block and phosphorylation of mSin1 T86 and Akt-S473 was monitored using western blotting at indicated timepoints after release. Left panel: western blots; Right panel: quantification of western blots with expression levels relative to the time point 0h. A. B. C and D each represent an individual experiment.

monitoring of the cell cycle progression and mitosis, with mSin1.2-eGFP and observed the localization of mSin1 and H2B across the cell cycle over 12.5 h using a spinning disc confocal microscope. Of the four analyzed cells expressing mSin1.2-eGFP before mitosis, 100% displayed generally low mSin1.2 expression levels and exclusion of mSin1.2 from the nucleus. Two of those cells underwent mitosis and, following cytokinesis, showed strong
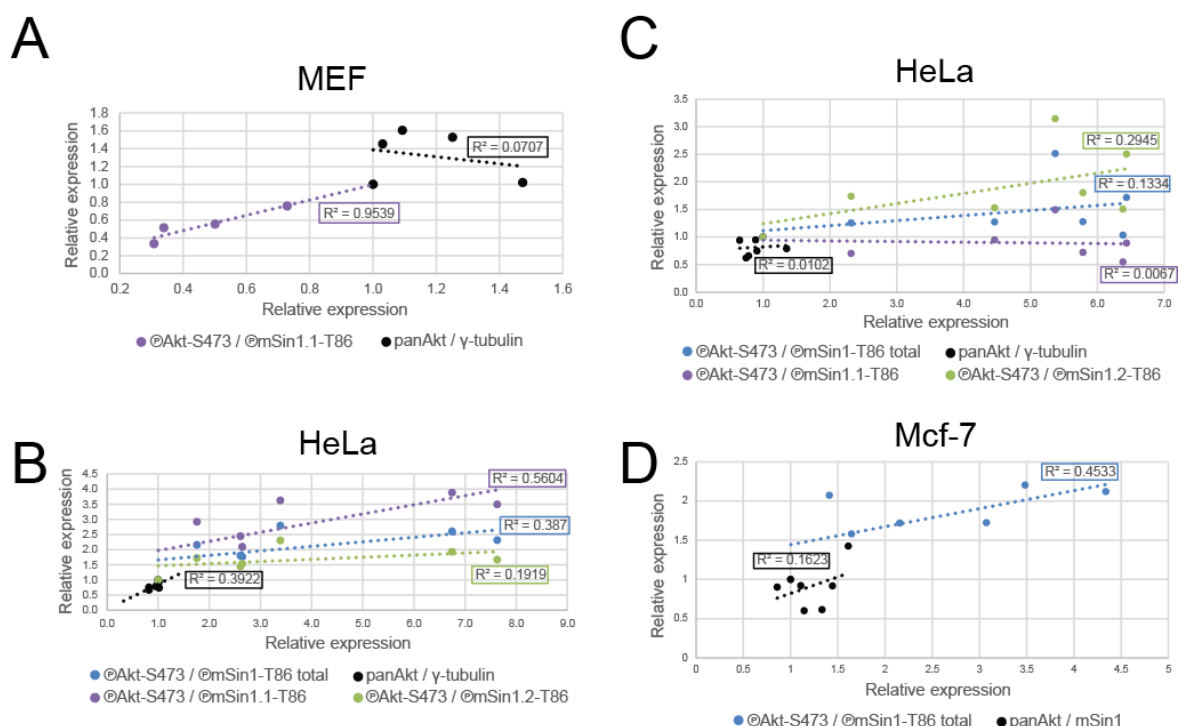
Figure 6: **Phosphorylation of mSin1 T86 and Akt S473 appear to correlate during the cell cycle**
Correlation analysis of western blot quantifications in Figure 5. The x and y axis are the relative expression levels of indicated proteins/phosphorylations plotted against eachother. Dotted lines are trendlines according to the linear model. A. B. C and D each represent an individual experiment.

expression and marked accumulation of mSin1.2 in the nucleus and the PM. In agreement with that, of the six cells expressing mSin1.2-eGFP only after cytokinesis, 9 out of 12 of their progeny displayed a strong expression of mSin1.2 with marked accumulation in the nucleus and at the PM with the remaining 3 cells out of 12 displaying equal subcellular distribution. It is important to note that many (9 out of 12) cells died during the course of this experiment. As the binning function, which amplifies signal by reducing resolution, was not utilized, higher exposure times and laser power were necessary for imaging. In combination with the long–term nature of this experiment, imaging in three z-planes, and numerous regions this was likely the cause of death for the 78 out of 100 GFP-expressing cells. Future experimenters would be advised to use lower exposure times in combination with appropriate binning to prevent laser-induced cytotoxicity. Drawing definitive conclusions from this experiment is thus impossible but the observation that nuclear mSin1.2-eGFP accumulation changes from mitosis to G1 phase sparked our interest.

Therefore, we performed a similar experiment in which we additionally synchronized cells using double thymidine block, and imaged them after release. Although only 43% of the mSin1.2-eGFP expressing cells died, none of them underwent mitosis during the 13,5 h time

course, the culprit again likely being too high laser exposure. Most cells (24 out of 31) displayed a low- to medium expression of mSin1.2-eGFP and many (17 out of 31) displayed no accumulation of mSin1.2-eGFP in the nucleus from the start or reduction of nuclear mSin1.2 during the experiment (7 out of 31). Of the six cells with high mSin1.2-eGFP expression, five showed increased nuclear accumulation while the remaining one had reduced nuclear signal compared to the cytoplasm. Of these six high-expressing cells, five died quickly while the other one displayed declining overall GFP fluorescence over the time course. Interestingly, one cell started expression of mSin1-eGFP during the experiment and displayed lack of nuclear localization until the signal equally distributed across the cell, likely caused by the onset of early mitosis as judged by the nuclear marker. These results, albeit preliminary, are in line with the previous experiment and provide further evidence that mSin1.2 localization could be regulated in a cell cycle-dependent manner.

Even though the cells in these long-term imaging experiments were subject to stress, the results obtained collectively point to the possibility that mSin1 could be inhibited from entering the nucleus in later cell cycle stages (e.g. S and G_2 phases) while being highly imported in G1. Furthermore, it is possible that this effect is due to mSin1-T86 phosphorylation by Akt. Future studies are required to test whether these observations hold true under less stressful conditions and imaging of complete cell cycles would help to clarify the issue.

Discussion

In this study, we used a combination of fluorescence imaging and biochemistry to examine the intracellular localization of the obligate mTORC2 subunit mSin1 and investigated how phosphorylation of mSin1 on T86 and T389, sites reported in earlier studies, could affect intracellular targeting of mTORC2.

We first tested whether mSin1-eGFP incorporated into functional mTORC2, in order to rule out that the C-terminal GFP tag used in this study could interfere with mTORC2 complex assembly and/or activity. Our results using GFP-pull-down and kinase assays clearly demonstrate that the GFP-tag neither interferes with complex assembly for mSin1 isoforms 1, 2 and 5, nor has any apparent effect on mTORC2 kinase activity (tested using mSin1 isoform 2). This is also in line with previous reports (Frias et al. 2006; Gaubitz et al. 2015) in

human and yeast cells, respectively, which show that C-terminal tags or truncation of the C-terminal PH domain had no effect on complex assembly, even when studied using EM (Gaubitz et al. 2015). It is important to mention, however, that overexpression of mSin1-eGFP will likely result in only a fraction of GFP-tagged molecules being a part of full mTORC2. It is, therefore, impossible to use mSin1-eGFP alone as a proxy for the localization of mTORC2.

Our data on intracellular localization of GFP-tagged mSin1 isoforms clearly demonstrate that the PH domain mediates its membrane binding. This is in line with a previous study showing the lack of membrane binding of EGFP-Sin1ΔPH in BHK cells (Schroder et al. 2007). Furthermore, PH-domain truncation in the yeast mSin1 ortholog, Avo1, induced cell death in the haploid cells, which was rescued using a different membrane anchor (Berchtold and Walther 2009). Furthermore, localization of mSin1-GFP at the plasma membrane and various endosomal vesicles is in line with the results of our recent study using a reporter of endogenous mTORC2 activity. This study demonstrated that in cells endogenous mTORC2 activity is present at the plasma membrane, outer mitochondrial membranes and a population of early- and late endosomes (Ebner, Sinkovics et al, 2017). With the notable exception of mitochondrial membranes, these data are in agreement with mSin1-eGFP membrane localization reported here and suggest that mSin1 targets mTORC2 to these cellular membranes via its PH domain.

mSin1 contains two AGC kinase consensus motifs and was reported to be phosphorylated on either T86 and/or T398 by the AGC kinases Akt and/or S6K (Liu et al. 2013; Humphrey, Yang et al. 2013; Yang et al. 2015). Although there is currently a controversy regarding the identity of the kinase responsible for phosphorylation of these residues, we examined the possible effects of these phosphorylation events on mSin1 localization using phosphomimetic mutations.

Incorporation of the T362E phosphomimetic mutation in mSin1.2 prevented its accumulation at the plasma membrane and on subcellular vesicles. Furthermore, co-expression of mSin1 with constitutively active S6K, but not myristoylated Akt1 or kinase inactive S6K1 had a similar effect on mSin1 localization, suggesting that phosphorylation of the T362 site in mSin1.2 could result in its dissociation from the membrane. Importantly, co-expression of constitutively active S6K1 with the non-phosphorylatable mSin1-T362A mutant prevented this membrane dissociation effect. These results indicate that S6K1 rather than

Akt is the kinase responsible for Sin1 membrane dissociation and that this is likely to be mediated by phosphorylation of the mSin1 PH-domain phosphosite (T362 in isoform 2).

Next, we examined the potential effect of T86 phosphorylation on mSin1 localization. T86 is located in the predicted bipartite NLS, and we hypothesized that its phosphorylation could interfere with nuclear-cytoplasmic shuttling of mSin1. Indeed, the T86E phosphomimetic mutant displayed less nuclear staining than WT mSin1, suggesting that T86 phosphorylation could help retain mSin1 in the cytosol.

There is conflicting evidence in the literature regarding the effect of mSin1 phosphorylation on the assembly and activity of mTORC2. Liu et al. (2013) suggested that dual phosphorylation of mSin1-T86 and T398 results in mTORC2 disassembly. The authors support this conclusion by using a dual T86E/T398E phosphomimetic mutant of mSin1 and gel-filtration assays with their N-terminally tagged mSin1.1. In contrast, other studies that used biochemistry on endogenous proteins for their research reported that phosphorylation of mSin1 on T86 by Akt resulted in increased activity of mTORC2 (Humphrey, Yang et al. (2013); Yang et al. (2015).

To test whether phosphorylation on these sites interfered with complex assembly, we used mSin1.2$^{T86E-T398E}$-eGFP in a preliminary experiment. Here, we were able to pull down the full mTORC2 complex from HEK293T cells (n=1 & data not shown). Similarly, mSin1.2$^{WT/T362E}$-eGFP was also a part of the fully assembled, active mTORC2 complex, arguing against the data of Liu et al. (2013). While the reasons for this controversy remain unclear, it is possible that the effect observed by Liu et al. (2013) was due to the fact that they used N-terminally tagged mSin1. A previous report mentioned that N-terminal myc-tagged mSin1 did not incorporate into mTORC2 (Frias et al. 2013), suggesting that the N-terminus is important for complex formation. As the C-terminally myc-tagged mSin1.4, which lacks the first 192 amino acids compared to the full-length isoform 1, was not able to co-IP mTOR or Rictor in a previous study (Frias et al. 2006) and the same was observed in a preliminary experiment with mSin1.4-eGFP in our lab, this suggests that the N-terminal fusion of mSin1 may interfere with its assembly into mTORC2. Taken together, it is possible that N-terminal mSin1 tags, which do not disassemble the mTORC2 completely, solely weaken complex interactions and eventually lead to disassembly of mTORC2 when in conjunction with phosphomimetic T86E and T398E mutations or phosphorylation on these sites. As there is no experimental evidence for this notion, the reasons for this discrepancy

remain unclear. This deficiency highlights the importance of further research on this subject in order to resolve this controversy.

Taken together, our conclusions allowed us to formulate the following model of how mSin1 phosphorylation could dynamically regulate subcellular localization of mTORC2. The PH domain of mSin1 mediates membrane targeting of mTORC2. Phosphorylation of T398 in mSin1.1 (T362 in mSin1.2) by S6K1 results in displacement of mTORC2, and thus its activity, from cellular membranes, thereby providing a mechanism for negative feedback from mTORC1 to mTORC2. mSin1.5, which lacks the PH domain, is thus not membrane-bound and likely performs a distinct function in a membrane-independent fashion. Furthermore, mSin1-T86 phosphorylation by Akt would hamper import of mSin1/mTORC2 into the nucleus and thus increase availability and activity of mTORC2 in non-nuclear compartments.

Our proposed model provides a possible mechanism as to how mTORC2 localization could be linked to its function and be regulated in the cellular context. Since mTORC1 localization is tightly coupled to its regulation and mTORC2 plays its part in mTORC1 activation, this form of regulation may also be applicable for mTORC2. Importantly, our model provides an alternative mechanism for the negative feedback from mTORC1 to mTORC2 via S6K and mSin1, which has been suggested earlier (Liu et al. 2013). It is important to note that S6K has been shown to phosphorylate Rictor on T1135, which did not change mTORC2 kinase activity, while T1135A mutation led to an increase in Akt-S473 phosphorylation (Dibble et al. 2009). The combination of mSin1.2-T362 and Rictor T1135 phosphorylation by S6K could be an important factor in negative regulation of mTORC2 and should be investigated further. In line with the possible role of S6K-mediated phosphorylation of the mTORC2 components are the data from a previous report (Rosner and Hengstschläger 2008) showing that 24 h rapamycin treatment, which also inhibits S6K activity, led to de-phosphorylation of mSin1 and Rictor, as judged by shift of their electrophoretic mobility. As there are 19 known candidate phosphorylation sites in mSin1 (according to PhosphoSitePlus), it is possible that many of these sites are dephosphorylated under the non-physiological conditions of long-term rapamycin treatment, which would not necessarily all be accounted for by S6K. Additionally, other posttranslational modifications could be influencing the electrophoretic mobility of mSin1 and Rictor. Lastly, long-term rapamycin treatment interferes with mTORC2 complex assembly (Sarbassov et al. 2006) and thus could subject mSin1 and Rictor to de-phosphorylation by cellular phosphatases, and

therefore maybe not be physiologically relevant. Together, this limits the implications the study of Rosner and Hengstschläger (2008) has on our model, but sparks interest for further research: in our model, we would expect at least mSin1-T362 to be unphosphorylated upon S6K inhibition.

At the same time, the aforementioned study is also, to our knowledge, the only one that investigated mTORC2 components in the nucleus (Rosner and Hengstschläger 2008). Importantly, the researchers show that mTORC components mSin1, Rictor and mTOR localize to the nucleus by subcellular fractionation, indicating a currently unknown role of mTORC2 in the nucleus (Rosner and Hengstschläger 2008).

Furthermore, their data show the reduction of mSin1.1 and rictor in the nucleus with a simultaneous increase in the cytoplasm upon 24 h rapamycin treatment. This data is consistent with our model, as rapamycin increases Akt activity (reviewed in Saxton and Sabatini 2017), which would lead to mSin1-T86 phosphorylation, thereby explaining the reduction in nuclear mSin1. At the same time, S6K would not be active and thus not remove mSin1/mTORC2 from the membrane compartments, likely further reducing mSin1 availability for nuclear import. Importantly, these effects could also be due to non-physiological effects of long-term rapamycin treatment and thus may not represent a physiologically relevant mechanism.

A possible caveat in our model is the lack of evidence for the situation where mSin1 is phosphorylated on both T86 and T398 (or T362 in isoform 2). From our model, we hypothesize that dually phosphorylated mSin1 is removed from membrane compartments due to T398/362 phosphorylation. This would result in mSin1/mTORC2 accumulation in the cytoplasm, which has not yet been monitored. It would likely be helpful to investigate mSin1-[T86E-T398E]-eGFP localization in cells in order to further test this model. How, when, and where mSin1 is phosphorylated and de-phosphorylated and how this influences mTORC2 assembly and function has to be further investigated.

Even though our preliminary result provides evidence against the model where mSin1 dual phosphorylation leads to complex disassembly (Liu et al. 2013), it would partly fit to our model as it would provide a mechanism for negative feedback. mTORC2 components could then be recycled or degraded in the cytoplasm. However, how exactly this could function in cells remains to be investigated. Finally, it would be important to perform mTORC2 formation experiments with different mSin1 isoforms and T86E-T398E double

phosphomimetics with tags on C- or N-terminus to determine if the complex disassembly reported by Liu et al. (2013) is an effect of the tag or the mSin1 isoform. Alternatively, investigating actual phosphorylation of mSin1.1-T86 and -T398/362 on pulled down mTORC2 would help to further understand the regulation of mSin1 and mTORC2.

In conclusion, we would suggest to perform more biological replicates and compile more data of the experiments performed in this study in order to strengthen the results and test our hypotheses. Thus, we suggest following experiments: First, in order to test the role of T86 in nuclear import of mSin1, it would be interesting to investigate mSin1 binding to nuclear import proteins such as importin-α under phosphomimetic/mutant/endogenous phosphorylation state by co-IP experiments. Second, the presence of mSin1-T398 phosphorylation site reported previously by Liu et al. (2013) should be reproduced using the endogenous protein. Third, it could be helpful to observe mSin1-T86 and/or -T398/362 phosphomimetics/mutants during the complete cell cycle to determine possible stages of nuclear import/export, or differential cellular localization. Lastly, it would be important to investigate mTORC2 formation and activity in the context of different mSin1 isoforms and Rictor phosphomimetics/mutants on various sites. Taken together, the research of mSin1 post-translational modification and their implications for cellular physiology are just at their beginning and future studies will uncover important regulatory mechanisms and functions of mSin1 in the mTORC2 context.

Methods & Materials

The Methods and Material section partly overlaps with our recently published paper (Ebner, Sinkovics et al.2017) and is thus referenced here.

Antibodies and Reagents

Rabbit Akt[pSer473] 193H12 (4058), rabbit mTOR 7C10 (2983), rabbit pan-Akt 11E7 (4685), rabbit GFP (D5.1), rabbit γ-tubulin (5886), anti-mouse Alexa Fluor® 647 Conjugate (4410), anti-mouse HRP-linked (7076) and anti-rabbit HRP-linked (7074) antibodies were from Cell Signaling Technology. Mouse RICTOR 7B3 (MA-5-15681) and HA11 biotin conjugated (2-2.2.14) antibodies were from Thermo Fisher Scientific. Mouse Sin1 1C7.2 (05-1044) antibody was from EMD Millipore. GFP-Trap A (gta-20) was from Chromo-Tek. Recombinant human

insulin (I2643) was from Sigma-Aldrich. Torin1 (10997) was from Cayman Chemicals. Thymidine (6060) was from EMD Millipore.

Cell culture

HEK293T cells were obtained from ATCC; HeLa and Mcf-7cells were gifts from R. Foisner (Max F. Perutz Laboratories, Vienna, Austria) and N. Huttary (Medical University of Vienna, Vienna, Austria), respectively. HeLa Kyoto cells were gifted by C. Blaukopf from D.Gerlich's Lab (Institute of Molecular Biotechnology Vienna, Austria). All cells were maintained in DMEM supplemented with 10% heat-inactivated FBS, 1 mM l-glutamine, 100 U/ml penicillin, and 100 μg/ml streptomycin at 37°C and 5% CO_2. Cell transfections were performed transiently using 1 mg/ml polyethyleneimine solution at a ratio of 1 μg DNA per 3 μl polyethylenimine.

Immunoprecipitation, *In Vitro* Kinase Assay, and Western Blotting

For immunoprecipitation experiments, the cells were lysed over 30 min in ice-cold 0.3% CHAPS buffer (40 mM Hepes, pH 7.4, 120 mM NaCl, 1 mM EDTA, and 0.3% CHAPS; containing Complete Mini, EDTA-free Protease Inhibitor Cocktail (ROCHE) and Phosphatase Inhibitor Mini (PIERCE)), which preserves mTORC2 integrity (Sarbassov et al. 2004; Frias et al. 2006). The lysates were cleared from cellular debris by centrifugation at 14000g for 10 min at 4°C. In Immunoprecipitation experiments, the proteins were then pulled down from the cleared lysates using GFP-Trap beads (ChromoTek) following the manufacturer's protocol. In *in vitro* kinase experiments the randomly growing cells were treated with 100 nM (final concentration) insulin before lysis. The kinase activity of the immunoprecipitated mTORC2 towards dephosphorylated recombinant full length human Akt1 (a kind gift from I. Lučić, Max F. Perutz Laboratories, Vienna, Austria) was assayed by incubating the IP fractions with Akt for 1 h at 37°C with gentle shaking. In cell cycle experiments, cells were lysed with 1% NP40, protein concentration in cleared lysates was measured by Bradford assay, and the loading samples were adjusted to have equal protein concentrations. Proteins were separated in 8% SDS-PAGE gels and electroblotted onto nitrocellulose membrane using the semi-dry procedure. Primary antibodies were visualized using HRP-conjugated secondary antibodies and ECL Select WB detection reagent (GE-Healthcare). Chemiluminiscence signal

was recorded using the FusionFX system (Peqlab). The band intensity was quantified using the ImageJ GelAnalyzer script in ImageJ (National Institutes of Health).

Microscopy and image analysis

Cells were grown on glass cover slips, fixed with 4% formaldehyde, stained with DAPI (4',6-diamidino-2-phenylindole) and mounted onto microscope slides using Mowiol4-88. In Figures 3B and C, cells were additionally, before staining with DAPI, permeabilized with 0.1% Triton-X100, blocked with 5% goat serum, and S6K1/Akt1 were detected using purified anti-HA11 antibody and anti-mouse Alexa Fluor® 647 Conjugated antibody. Confocal laser-scanning microscopy of fixed samples was performed using the Zeiss LSM700 or LSM710 system with a 63×/NA 1.4 oil immersion objective and the Zeiss Zen software. Images were then processed and analysed using ImageJ. All adjustments were equally applied across the entire image. For live-cell imaging we used the LIVE spinning-disk confocal microscopy system (Visitron Systems) equipped with an electron-multiplying charge-coupled device camera (Evolve; Photometrics), a 63×/NA 1.4 oil immersion objective, an environmental control unit (5% CO2, 37°C) and using the VisiView software (Visitron Systems). Imaging medium was DMEM once with, once without phenol-red, supplemented with 1 mM l-glutamine, 100 U/ml penicillin, and 100 μg/ml streptomycin and 10% FBS.

Figure 4: Quantification of signal ratio was done with ImageJ by creating masks of the nucleus and cytoplasm, measuring the average GFP signal intensity in those two compartments and calculating the nuclear/cytoplasmic GFP intensity ratio. Statistics: The box plot in Figure 4 was created with an online tool (http://boxplot.tyerslab.com/) (Spitzer et al. 2014) using data from one experiment and indicated number of analyzed cells. Statistical significance was calculated with a one tailed built-in Excel 2013 t-Test: Two-Sample Assuming Unequal Variances.

Detailed Figure 4 ImageJ analysis: The cells were segmented in each image by manually encircling and cropping the ROI (region of interest) defined by the outer border in the green channel (representative of cellular borders as sin1 localizes throughout the cells. The *first macro* was then used to create the image files for measurement and thresholding (8-bit). Then, the green and blue channel (GFP and DAPI) 8-bit images were visually thresholded, and the holes were filled using imaging opening followed by image closing binary operations. Masks of green and blue channel were created by analyzing particles, using the ROI and

individual particle sizes to only represent correct signal. Then the *Second macro* was used to firstly create the mask of only cytoplasm by subtracting total from nuclear green signal, secondly creating 32-bit images in order to set the background 0 to NaN (not-a-number) values and thirdly measuring the average intensity of GFP channel signal in nucleus and cytoplasm by using the masks and the original image. These steps were done individually for each cell.

ImageJ macros:

First macro

```
setSlice(1);
rename("source.tif");
selectWindow("source.tif");
run("Duplicate...", "title=blue.tif duplicate channels=1");
rename("blue.tif");
selectWindow("source.tif");
setSlice(3);
run("Duplicate...", "title=green.tif duplicate channels=3");
selectWindow("green.tif");
run("Duplicate...", "title=[8bit green-1.tif]");
selectWindow("blue.tif");
run("Duplicate...", "title=[8bit blue-1.tif]");
selectWindow("8bit green-1.tif");
run("8-bit");
run("Duplicate...", "title=[8bit green thresh.tif]");
selectWindow("8bit blue-1.tif");
run("8-bit");
run("Duplicate...", "title=[8bit blue thresh.tif]");
selectWindow("source.tif");
roiManager("Add");
```

Second macro

```
selectWindow("Mask of 8bit green thresh.tif");
roiManager("Select", 0);
selectWindow("Mask of 8bit blue thresh.tif");
roiManager("Select", 0);
run("Set Measurements...", "mean standard redirect=None decimal=3");
selectWindow("green.tif");
resetMinAndMax();
imageCalculator("AND create", "Mask of 8bit green thresh.tif", "green.tif");
selectWindow("Result of Mask of 8bit green thresh.tif");
roiManager("Select", 0);
imageCalculator("AND create", "Mask of 8bit blue thresh.tif", "green.tif");
selectWindow("Result of Mask of 8bit blue thresh.tif");
roiManager("Select", 0);
imageCalculator("Subtract create 32-bit", "Result of Mask of 8bit green thresh.tif","Result of Mask of 8bit blue thresh.tif");
selectWindow("Result of Result of Mask of 8bit green thresh.tif");
```

```
roiManager("Select", 0);
run("Set Zero to NaN");
selectWindow("Result of Mask of 8bit blue thresh.tif");
imageCalculator("Copy create 32-bit", "Result of Mask of 8bit blue thresh.tif","Result of Mask of 8bit blue thresh.tif");
roiManager("Select", 0);
run("Set Zero to NaN");
selectWindow("Result of Result of Mask of 8bit blue thresh.tif");
run("Measure");
selectWindow("Result of Result of Mask of 8bit green thresh.tif");
run("Measure");
  dir = getDirectory("image");
  name = getTitle;
  index = lastIndexOf(name, ".");
  if (index!=-1) name = substring(name, 0, index);
  name = name + ".txt";
  saveAs("Measurements", dir);
  print(dir);
// get image IDs of all open images
dir = getDirectory("Choose a Directory");
ids=newArray(nImages);
for (i=0;i<nImages;i++) {
    selectImage(i+1);
    title = getTitle;
    print(title);
    ids[i]=getImageID;
    saveAs("tiff", dir+title);}
if (isOpen("Results")) {
    selectWindow("Results");
    run("Close");}
if (isOpen("ROI Manager")) {
    selectWindow("ROI Manager");
    run("Close"); }
if (isOpen("Log")) {
    selectWindow("Log");
    run("Close");}
 macro "Close All Windows" {
    while (nImages>0) {
      selectImage(nImages);
      close(); } }
```

Cell synchronization

For the double thymidine block experiments, the cells were transfected with indicated
constructs and blocked in the cell cycle by usage of the following protocol at appropriate
density. Cells were blocked with 2 mM thymidine for 16 h, washed 2x with warm DBPS and

released in growth medium, grown for 8 hours, blocked as before for 16 h, washed out 2x as before and released in growth medium or imaging growth medium.

Sequences and cloning

General cloning and sequencing were done according to standard molecular biology protocols. The mSin1.1 sequence was derived from a HeLa cDNA library which was kindly provided by Daniel Elsner (Department for Structural and Computational Biology; Max F. Perutz Laboratories, Austria) and cloned into the mammalian expression vector eGFP-N1. Other mSin1 Isoforms and their mutations were derived from this construct by PCR mutagenesis. Sequencing with following reference sequences: CCDS48020.1 (mSin1.1), CCDS35140.1 (mSin1.2) and CCDS48020.1 (mSin1.5) was used to confirm correct clones. These sequences translated into the uniprot (http://www.uniprot.org/uniprot/Q9BPZ7) amino acid sequences of the respective mSin1 isoforms. mCherry-KRas4B[C30] construct used in Figure 3A had an N-terminal FKBP tag linked to mCherry and the 30 C-terminal residues of KRas4B. Myristoylated Akt1 in Figures 3B and C was a gift from Rajeshwari Meli from the F. Propst lab (Max F. Perutz Laboratories, Vienna, Austria) and contained the N-terminal Src myristoylation site, a C-terminal HA tag and a S473F mutation. Constitutively active and kinase dead S6K1 were obtained from Addgene (Plasmid #8991) and (Plasmid #8986).

References

Berchtold, D., and T. C. Walther. "Torc2 Plasma Membrane Localization Is Essential for Cell Viability and Restricted to a Distinct Domain." *Mol Biol Cell* 20, no. 5 (2009): 1565-75.

Betz, C., and M. N. Hall. "Where Is Mtor and What Is It Doing There?" *J Cell Biol* 203, no. 4 (2013): 563-74.

Betz, C., D. Stracka, C. Prescianotto-Baschong, M. Frieden, N. Demaurex, and M. N. Hall. "Feature Article: Mtor Complex 2-Akt Signaling at Mitochondria-Associated Endoplasmic Reticulum Membranes (Mam) Regulates Mitochondrial Physiology." *Proc Natl Acad Sci U S A* 110, no. 31 (2013): 12526-34.

Boulbes, D. R., T. Shaiken, and D. Sarbassov dos. "Endoplasmic Reticulum Is a Main Localization Site of Mtorc2." *Biochem Biophys Res Commun* 413, no. 1 (2011): 46-52.

Dibble, C. C., J. M. Asara, and B. D. Manning. "Characterization of Rictor Phosphorylation Sites Reveals Direct Regulation of Mtor Complex 2 by S6k1." *Mol Cell Biol* 29, no. 21 (2009): 5657-70.

Ebner, M., B. Sinkovics, M. Szczygiel, D. W. Ribeiro, and I. Yudushkin. "Localization of Mtorc2 Activity inside Cells." *J Cell Biol*, (2017).

Frias, M. A., C. C. Thoreen, J. D. Jaffe, W. Schroder, T. Sculley, S. A. Carr, and D. M. Sabatini. "Msin1 Is Necessary for Akt/Pkb Phosphorylation, and Its Isoforms Define Three Distinct Mtorc2s." *Curr Biol* 16, no. 18 (2006): 1865-70.

Gaubitz, C., T. M. Oliveira, M. Prouteau, A. Leitner, M. Karuppasamy, G. Konstantinidou, D. Rispal, S. Eltschinger, G. C. Robinson, S. Thore, R. Aebersold, C. Schaffitzel, and R. Loewith. "Molecular Basis of the Rapamycin Insensitivity of Target of Rapamycin Complex 2." *Mol Cell* 58, no. 6 (2015): 977-88.

Humphrey, S. J., G. Yang, P. Yang, D. J. Fazakerley, J. Stockli, J. Y. Yang, and D. E. James. "Dynamic Adipocyte Phosphoproteome Reveals That Akt Directly Regulates Mtorc2." *Cell Metab* 17, no. 6 (2013): 1009-20.

Lange, A., R. E. Mills, C. J. Lange, M. Stewart, S. E. Devine, and A. H. Corbett. "Classical Nuclear Localization Signals: Definition, Function, and Interaction with Importin Alpha." *J Biol Chem* 282, no. 8 (2007): 5101-5.

Liu, P., M. Begley, W. Michowski, H. Inuzuka, M. Ginzberg, D. Gao, P. Tsou, W. Gan, A. Papa, B. M. Kim, L. Wan, A. Singh, B. Zhai, M. Yuan, Z. Wang, S. P. Gygi, T. H. Lee, K. P. Lu, A. Toker, P. P. Pandolfi, J. M. Asara, M. W. Kirschner, P. Sicinski, L. Cantley, and W. Wei. "Cell-Cycle-Regulated Activation of Akt Kinase by Phosphorylation at Its Carboxyl Terminus." *Nature* 508, no. 7497 (2014): 541-5.

Liu, P., W. Gan, Y. R. Chin, K. Ogura, J. Guo, J. Zhang, B. Wang, J. Blenis, L. C. Cantley, A. Toker, B. Su, and W. Wei. "Ptdins(3,4,5)P3-Dependent Activation of the Mtorc2 Kinase Complex." *Cancer Discov* 5, no. 11 (2015): 1194-209.

Liu, P., W. Gan, H. Inuzuka, A. S. Lazorchak, D. Gao, O. Arojo, D. Liu, L. Wan, B. Zhai, Y. Yu, M. Yuan, B. M. Kim, S. Shaik, S. Menon, S. P. Gygi, T. H. Lee, J. M. Asara, B. D. Manning, J. Blenis, B. Su, and W. Wei. "Sin1 Phosphorylation Impairs Mtorc2 Complex Integrity and Inhibits Downstream Akt Signalling to Suppress Tumorigenesis." *Nat Cell Biol* 15, no. 11 (2013): 1340-50.

Oh, W. J., C. C. Wu, S. J. Kim, V. Facchinetti, L. A. Julien, M. Finlan, P. P. Roux, B. Su, and E. Jacinto. "Mtorc2 Can Associate with Ribosomes to Promote Cotranslational Phosphorylation and Stability of Nascent Akt Polypeptide." *EMBO J* 29, no. 23 (2010): 3939-51.

Pan, D., and Y. Matsuura. "Structures of the Pleckstrin Homology Domain of Saccharomyces Cerevisiae Avo1 and Its Human Orthologue Sin1, an Essential Subunit of Tor Complex 2." *Acta Crystallogr Sect F Struct Biol Cryst Commun* 68, no. Pt 4 (2012): 386-92.

Rosner, M., and M. Hengstschlager. "Cytoplasmic and Nuclear Distribution of the Protein Complexes Mtorc1 and Mtorc2: Rapamycin Triggers Dephosphorylation and Delocalization of the Mtorc2 Components Rictor and Sin1." *Hum Mol Genet* 17, no. 19 (2008): 2934-48.

Sarbassov, D. D., S. M. Ali, D. H. Kim, D. A. Guertin, R. R. Latek, H. Erdjument-Bromage, P. Tempst, and D. M. Sabatini. "Rictor, a Novel Binding Partner of Mtor, Defines a Rapamycin-Insensitive and Raptor-Independent Pathway That Regulates the Cytoskeleton." *Curr Biol* 14, no. 14 (2004): 1296-302.

Sarbassov, D. D., S. M. Ali, S. Sengupta, J. H. Sheen, P. P. Hsu, A. F. Bagley, A. L. Markhard, and D. M. Sabatini. "Prolonged Rapamycin Treatment Inhibits Mtorc2 Assembly and Akt/Pkb." *Mol Cell* 22, no. 2 (2006): 159-68.

Saxton, R. A., and D. M. Sabatini. "Mtor Signaling in Growth, Metabolism, and Disease." *Cell* 168, no. 6 (2017): 960-976.

Schroder, W., G. Bushell, and T. Sculley. "The Human Stress-Activated Protein Kinase-Interacting 1 Gene Encodes Jnk-Binding Proteins." *Cell Signal* 17, no. 6 (2005): 761-7.

Schroder, W., N. Cloonan, G. Bushell, and T. Sculley. "Alternative Polyadenylation and Splicing of Mrnas Transcribed from the Human Sin1 Gene." *Gene* 339, (2004): 17-23.

Schroder, W. A., M. Buck, N. Cloonan, J. F. Hancock, A. Suhrbier, T. Sculley, and G. Bushell. "Human Sin1 Contains Ras-Binding and Pleckstrin Homology Domains and Suppresses Ras Signalling." *Cell Signal* 19, no. 6 (2007): 1279-89.

Spitzer, M., J. Wildenhain, J. Rappsilber, and M. Tyers. "Boxplotr: A Web Tool for Generation of Box Plots." *Nat Methods* 11, no. 2 (2014): 121-2.

Yang, G., D. S. Murashige, S. J. Humphrey, and D. E. James. "A Positive Feedback Loop between Akt and Mtorc2 Via Sin1 Phosphorylation." *Cell Rep* 12, no. 6 (2015): 937-43.

Yuan, Y., B. Pan, H. Sun, G. Chen, B. Su, and Y. Huang. "Characterization of Sin1 Isoforms Reveals an Mtor-Dependent and Independent Function of Sin1gamma." *PLoS One* 10, no. 8 (2015): e0135017.

Zinzalla, V., D. Stracka, W. Oppliger, and M. N. Hall. "Activation of Mtorc2 by Association with the Ribosome." *Cell* 144, no. 5 (2011): 757-68.

German Abstract / Zusammenfassung

Obwohl vorangegangene Studien den mechanistic target of ramapamycin complex 2 (mTORC2) mit Zellulären Wachstums-signaltransduktionswegen und Überleben in Verbindung gebracht haben steht die Untersuchung seiner Regulation und Funktion erst am Anfang. Die obligate mTORC2 Komponente mSin1 ist mit seiner pleckstrin homology (PH) domäne, welche in zwei der drei mTORC2 formenden Isoformen vorkommt, der Hauptkandidat für die Zielbestimmung der intrazellulären Lokalisierung des Komplexes. In dieser Studie haben wir die Lokalisierung von eGFP-markierten mSin1 Isoformen in Zellen mithilfe von Konfokalmikroskopie untersucht und den Einfluss von phospomimetischen und phosphomutanten mutationen in den zwei AGC Kinase Motiven in mSin1, T86 und T398 (T362 in Isoform 2) darauf erforscht. Wir zeigen, dass die mSin1 PH domäne notwendig für seine Membranbindung ist und, dass die phosphorylierung von T362, von S6K1, die Membranassoziierung zu verhindern scheint. Außerdem bieten wir Hinweise welche andeuten, dass mSin1-T86 phosphorylierung den Import in den Nukleus behindert.